Inversion of qP wave travel times: synthetic study [1]

JingSong Liu* and **Ivan Pšenčík****

* *Institute of Geophysics, Chinese Academy of Sciences, P. O. Box 9701, 100101 Beijing, China; e-mail: jsliu@mail.c-geos.ac.cn*

** *Geophysical Institute, Acad.Sci.of Czech Republic, Boční II, Praha 4, Czech Republic; e-mail: ip@ig.cas.cz*

Abstract

An iterative procedure to determine lateral variation of 21 elastic parameters from qP wave travel times is proposed. The procedure consists of two steps. In the first step, an isotropic starting model is updated using formulae for weak anisotropy. In this way, 15 qP wave weak anisotropy (WA) parameters are determined. The WA parameters serve as a basis for an estimate of all 21 elastic parameters, which are iteratively updated until the difference between observed and calculated travel times stops to vary. No a priori assumptions about heterogeneity and anisotropy of a model are made except the variation of elastic parameters with respect to spatial coordinates in the model box is assumed to be trilinear.

The procedure is tested on a synthetic multi-azimuthal multiple-source offset VSP experiment. Travel times were picked from noiseless qP wave synthetics generated by sources distributed along 6 profiles itersecting at the mouth of a borehole with receivers. The model considered is vertically inhomogeneous of hexagonal symmetry, with nearly horizontal axis of symmetry. The model may thus simmulate a cracked medium with a slightly tilted system of vertical parallel cracks. The SVD technique is used for solving the system of linear equations resulting from the condition of minimization of the object function. Due to insufficient illumination of the studied structure, the inversion process is surprisingly slow. At least for qP waves, however, it converges to elastic parameters of the true model. In case of qS waves, the resulting phase velocities roughly show a proper angular variation but the phase velocity surfaces based on inverted data have a nearly constant offset from the true surfaces. The experiment shows that a single iteration is insufficient for accurate recovery of the structure.

Introduction

In most attempts of tomographic reconstruction in anisotropic media certain limiting assumptions were made in order to reduce the number of parameters to be inverted. For

[1]Seismic Waves in Complex 3-D Structures, Report 8 (Department of Geophysics, Charles University, Prague 1999), pp.27-46

example, Chapman and Pratt (1992) considered a general anisotropy but concentrated only on data collected in a 2D plane. Jech and Pšenčík (1992) made no such limitation but they considered the sought medium to be of hexagonal symmetry. In both cases the authors assumed that studied anisotropy is weak and thus only a single iteration, from an isotropic starting model to a resulting weakly anisotropic model was sufficient. In this contribution, we make no a priori assumptions about inhomogeneity and/or anisotropy of the medium except that a possible variation of elastic parameters with respect to spatial coordinates within a model is piece-wise trilinear. Since we wish to consider anisotropy of arbitrary strength, we propose an inversion procedure, which is iterative. As in the above mentioned papers, we start from an isotropic medium but we continue in updating of obtained anisotropic models in subsequent iterations. Let us mention that such an iterative approach has been used, for example, by Aggio (1994). A substantial difference from Aggio (1994) is that travel times of only qP waves are assumed to be available in this study.

We test the proposed procedure on a synthetic multi-azimuthal multiple-source offset VSP experiment. The travel times are picked from synthetics generated from 18 sources evenly distributed along 6 profiles, which cross each other at the mouth of the borehole with receivers. There are 13 receivers evenly distributed inside the borehole. In this way, we have 1404 travel time measurements.

The model is specified in a box, within which the variation of elastic parameters with spatial coordinates is trilinear. The aim of the inversion is to find 21 elastic parameters in each of 8 corners of the model box so that the object function Ω,

$$\Omega = \sum_{i=1}^{N} (\tau_i^{obs} - \tau_i^{cal})^2 \tag{1}$$

is minimized. Here τ_i^{obs} is the i-th of N observed travel times, τ_i^{cal} is the i-th of N travel times calculated in an assumed model. We thus search for 168 parameters. As stated above the procedure is divided into two steps: (a) inversion from an isotropic starting model into an anisotropic model; (b) iterative updating of an anisotropic model.

1st step: Inversion from isotropy to anisotropy

The perturbation formula for the qP wave travel times reads, see e.g. Červený (1982)

$$\tau = \tau^{iso} - \frac{1}{2} \int_{\tau_0}^{\tau} \alpha^{-2} \Delta a_{ijkl} n_i n_j n_k n_l d\xi = \tau^{iso} - \int_{\tau_0}^{\tau} \frac{\Delta c}{\alpha} d\xi . \tag{2}$$

Here τ^{iso} is the travel time between a source and a receiver in a background isotropic medium, Δa_{ijkl} is a tensor of deviations of density-normalized elastic parameters from their values in the background isotropic medium, Δc is a corresponding deviation of the qP wave phase velocity and α is the P wave velocity in the background isotropic medium. The integration is performed along a ray in the background medium, n_i being a unit vector

tangent to the ray representing a unit phase normal. According to Pšenčík & Gajewski (1998) the term $\Delta c/\alpha$ can be expressed as

$$\frac{\Delta c(n_m)}{\alpha} = \epsilon_z n_3^4 + 2n_3^3(\epsilon_{34} n_2 + \epsilon_{35} n_1) + n_3^2(\delta_x n_1^2 + \delta_y n_2^2 + 2\chi_z n_1 n_2)$$
$$+2n_3(\chi_x n_1^2 n_2 + \chi_y n_1 n_2^2 + \epsilon_{15} n_1^3 + \epsilon_{24} n_2^3) + \epsilon_x n_1^4 + \delta_z n_1^2 n_2^2$$
$$+\epsilon_y n_2^4 + 2\epsilon_{16} n_1^3 n_2 + 2\epsilon_{26} n_1 n_2^3, \tag{3}$$

where

$$\epsilon_x = \frac{A_{11} - \alpha^2}{2\alpha^2}, \quad \epsilon_y = \frac{A_{22} - \alpha^2}{2\alpha^2}, \quad \epsilon_z = \frac{A_{33} - \alpha^2}{2\alpha^2},$$
$$\delta_x = \frac{A_{13} + 2A_{55} - \alpha^2}{\alpha^2}, \quad \delta_y = \frac{A_{23} + 2A_{44} - \alpha^2}{\alpha^2}, \quad \delta_z = \frac{A_{12} + 2A_{66} - \alpha^2}{\alpha^2},$$
$$\chi_x = \frac{A_{14} + 2A_{56}}{\alpha^2}, \quad \chi_y = \frac{A_{25} + 2A_{46}}{\alpha^2}, \quad \chi_z = \frac{A_{36} + 2A_{45}}{\alpha^2},$$
$$\epsilon_{15} = \frac{A_{15}}{\alpha^2}, \quad \epsilon_{16} = \frac{A_{16}}{\alpha^2}, \quad \epsilon_{24} = \frac{A_{24}}{\alpha^2}, \quad \epsilon_{26} = \frac{A_{26}}{\alpha^2}, \quad \epsilon_{34} = \frac{A_{34}}{\alpha^2}, \quad \epsilon_{35} = \frac{A_{35}}{\alpha^2} \tag{4}$$

are the qP wave weak anisotropy (WA) parameters defined with respect to an arbitrary background P wave velocity α. An important advantage of using the WA parameters in this step of inversion is that they are all of the same order. All of the WA parameters represent a small correction to the parameters specifying the background isotropic medium.

Let us choose any of the WA parameters and denote it $\epsilon = \epsilon(x, y, z)$. We shall specify the parameter ϵ by values at grid points of a 3D grid. We denote by ϵ_{ijk} the value of ϵ at the grid point formed by intersection of x_i, y_j and z_k grid lines, $\epsilon_{ijk} = \epsilon(x_i, y_j, z_k)$. Between grid points, we use the trilinear interpolation

$$\epsilon(x, y, z) = \epsilon_{ijk} + A_{100}(x - x_i) + A_{010}(y - y_j) + A_{001}(z - z_k) + A_{110}(x - x_i)(y - y_j)$$
$$+A_{011}(y - y_j)(z - z_k) + A_{110}(x - x_i)(z - z_k) + A_{111}(x - x_i)(y - y_j)(z - z_k). \tag{5}$$

The coefficients A_{ijk} are defined as follows

$$A_{100} = \frac{\epsilon_{i+1jk} - \epsilon_{ijk}}{x_{i+1} - x_i}, \quad A_{010} = \frac{\epsilon_{ij+1k} - \epsilon_{ijk}}{y_{j+1} - y_j}, \quad A_{001} = \frac{\epsilon_{ijk+1} - \epsilon_{ijk}}{z_{k+1} - z_k},$$

$$A_{110} = \frac{\epsilon_{i+1j+1k} - \epsilon_{i+1jk} - \epsilon_{ij+1k} + \epsilon_{ijk}}{(x_{i+1} - x_i)(y_{j+1} - y_j)}, \quad A_{011} = \frac{\epsilon_{ij+1k+1} - \epsilon_{ij+1k} - \epsilon_{ijk+1} + \epsilon_{ijk}}{(y_{j+1} - y_j)(z_{k+1} - z_k)},$$

$$A_{101} = \frac{\epsilon_{i+1jk+1} - \epsilon_{i+1jk} - \epsilon_{ijk+1} + \epsilon_{ijk}}{(x_{i+1} - x_i)(z_{k+1} - z_k)},$$

$$A_{111} = \frac{\epsilon_{i+1j+1k+1} - \epsilon_{i+1j+1k} - \epsilon_{ij+1k+1} - \epsilon_{i+1jk+1} + \epsilon_{i+1jk} + \epsilon_{ij+1k} + \epsilon_{ijk+1} - \epsilon_{ijk}}{(x_{i+1} - x_i)(y_{j+1} - y_j)(z_{k+1} - z_k)}. \tag{6}$$

In order to minimize (1), we need to know the derivatives $\partial\tau/\partial\epsilon_{ijk}$ of travel times with respect to ϵ_{ijk}. Differentiating Eq.(2), we get

$$\frac{\partial\tau}{\partial\epsilon_{ijk}} = -\int_{\tau_0}^{\tau} \alpha^{-1}\frac{\partial\Delta c}{\partial\epsilon}\frac{\partial\epsilon}{\partial\epsilon_{ijk}}d\xi. \tag{7}$$

The derivative $\partial\Delta c/\partial\epsilon$ can be obtained by differentiating Eq.(3) with respect to the corresponding WA parameter. This yields

$$\frac{\partial\Delta c}{\partial\epsilon_x} = \alpha n_1^4, \quad \frac{\partial\Delta c}{\partial\epsilon_y} = \alpha n_2^4, \quad \frac{\partial\Delta c}{\partial\epsilon_z} = \alpha n_3^4,$$

$$\frac{\partial\Delta c}{\partial\delta_x} = \alpha n_1^2 n_3^2, \quad \frac{\partial\Delta c}{\partial\delta_y} = \alpha n_2^2 n_3^2, \quad \frac{\partial\Delta c}{\partial\delta_z} = \alpha n_1^2 n_2^2,$$

$$\frac{\partial\Delta c}{\partial\chi_z} = 2\alpha n_1 n_2 n_3^2, \quad \frac{\partial\Delta c}{\partial\chi_x} = 2\alpha n_1^2 n_2 n_3, \quad \frac{\partial\Delta c}{\partial\chi_y} = 2\alpha n_1 n_2^2 n_3,$$

$$\frac{\partial\Delta c}{\partial\epsilon_{15}} = 2\alpha n_1^3 n_3, \quad \frac{\partial\Delta c}{\partial\epsilon_{16}} = 2\alpha n_1^3 n_2, \quad \frac{\partial\Delta c}{\partial\epsilon_{24}} = 2\alpha n_2^3 n_3,$$

$$\frac{\partial\Delta c}{\partial\epsilon_{26}} = 2\alpha n_1 n_2^3, \quad \frac{\partial\Delta c}{\partial\epsilon_{34}} = 2\alpha n_2 n_3^3, \quad \frac{\partial\Delta c}{\partial\epsilon_{35}} = 2\alpha n_1 n_3^3. \tag{8}$$

The derivatives $\partial\epsilon/\partial\epsilon_{ijk}$ can be obtained by differentiating $\epsilon(x,y,z)$ in Eq.(5) with respect to ϵ_{ijk}. This yields

$$\frac{\partial\epsilon}{\partial\epsilon_{ijk}} = 1 - \frac{x-x_i}{x_{i+1}-x_i} - \frac{y-y_j}{y_{j+1}-y_j} - \frac{z-z_k}{z_{k+1}-x_k} + \frac{(x-x_i)(y-y_j)}{(x_{i+1}-x_i)(y_{j+1}-y_j)}$$

$$+\frac{(y-y_j)(z-z_k)}{(y_{j+1}-y_j)(z_{k+1}-z_k)} + \frac{(x-x_i)(z-z_k)}{(x_{i+1}-x_i)(z_{k+1}-z_k)} - \frac{(x-x_i)(y-y_j)(z-x_k)}{(x_{i+1}-x_i)(y_{j+1}-y_j)(z_{k+1}-z_k)},$$

$$\frac{\partial\epsilon}{\partial\epsilon_{i+1jk}} = \frac{x-x_i}{x_{i+1}-x_i} - \frac{(x-x_i)(y-y_j)}{(x_{i+1}-x_i)(y_{j+1}-y_j)}$$

$$-\frac{(x-x_i)(z-z_k)}{(x_{i+1}-x_i)(z_{k+1}-z_k)} + \frac{(x-x_i)(y-y_j)(z-x_k)}{(x_{i+1}-x_i)(y_{j+1}-y_j)(z_{k+1}-z_k)}, \tag{9}$$

etc.

2nd step: Iterative inversion from anisotropy to anisotropy

From the WA parameters found in the first step of inversion, we can construct approximate estimates of elastic parameters. The determination of parameters A_{11}, A_{22}, A_{33}, A_{15}, A_{16}, A_{24}, A_{26}, A_{34} and A_{35} is straightforward, see Eqs.(4). When seeking the remaining parameters, which appear in combinations in Eqs.(4), we can use various assumptions. Here we assume that

$$A_{44} = A_{55} = A_{66} = \frac{A_{11} + A_{22} + A_{33}}{9} \tag{10}$$

and A_{12}, A_{13} and A_{23} can then be easily determined from Eqs.(4). Further, we set

$$A_{45} = A_{46} = A_{56} = 0 \tag{11}$$

and again, the parameters A_{14}, A_{25} and A_{36} can be easily determined from Eqs.(4). In this way, we can construct complete stiffness matrix, which serves as an initial guess for the second step of inversion procedure. The initial medium is now generally inhomogeneous and anisotropic and all 21 elastic parameters are sought in the second and higher iterations.

The perturbation formula for travel time when the background medium is anisotropic reads, see Červený (1982), Jech and Pšenčík (1989)

$$\tau = \tau^{ani} - \frac{1}{2}\int_{\tau_0}^{\tau} \Delta a_{ijkl} p_i g_j g_k p_l d\xi = \tau^{ani} - \frac{1}{2}\int_{\tau_0}^{\tau} \Delta G d\xi, \tag{12}$$

Here τ^{ani} is the travel time between a source and a receiver in a background anisotropic medium determined during the previous iteration, p_i denote components of the slowness vector and g_i components of the unit polarization vector, both calculated along the ray in the background medium. The values p_i and g_i are automatically generated when a ray is calculated in an anisotropic medium by the program ANRAY (Gajewski and Pšenčík (1990).

The derivatives necessary for inversion, $\partial\Delta\tau/\partial A_{\alpha\beta,ijk}$, where $A_{\alpha\beta,ijk}$ is the value of the parameter $A_{\alpha\beta}$ at the grid point (x_i, y_j, z_k) and α, $\beta = 1, 2, .., 6$, read

$$\frac{\partial\tau}{\partial A_{\alpha\beta,ijk}} = -\frac{1}{2}\int_{\tau_0}^{\tau} \frac{\partial\Delta G}{\partial A_{\alpha\beta}} \frac{\partial A_{\alpha\beta}}{\partial A_{\alpha\beta,ijk}} d\xi. \tag{13}$$

The derivative $\partial\Delta G/\partial A_{\alpha\beta}$ can be obtained by taking into account the definition of ΔG in (12). We get

$$\frac{\partial\Delta G}{\partial A_{11}} = p_1^2 g_1^2, \quad \frac{\partial\Delta G}{\partial A_{22}} = p_2^2 g_2^2, \quad \frac{\partial\Delta G}{\partial A_{33}} = p_3^2 g_3^2,$$

$$\frac{\partial\Delta G}{\partial A_{12}} = 2p_1 p_2 g_1 g_2, \quad \frac{\partial\Delta G}{\partial A_{13}} = 2p_1 p_3 g_1 g_3, \quad \frac{\partial\Delta G}{\partial A_{23}} = 2p_2 p_3 g_2 g_3,$$

$$\frac{\partial\Delta G}{\partial A_{14}} = 2p_1 g_1 g_2 p_3 + 2p_1 g_1 g_3 p_2, \qquad \frac{\partial\Delta G}{\partial A_{15}} = 2p_1 g_1 g_1 p_3 + 2p_1 g_1 g_3 p_1,$$

$$\frac{\partial\Delta G}{\partial A_{16}} = 2p_1 g_1 g_1 p_2 + 2p_1 g_1 g_2 p_1, \qquad \frac{\partial\Delta G}{\partial A_{24}} = 2p_2 g_2 g_2 p_3 + 2p_2 g_2 g_3 p_2,$$

$$\frac{\partial \Delta G}{\partial A_{25}} = 2p_2g_2g_1p_3 + 2p_2g_2g_3p_1, \qquad \frac{\partial \Delta G}{\partial A_{26}} = 2p_2g_2g_1p_2 + 2p_2g_2g_2p_1,$$
$$\frac{\partial \Delta G}{\partial A_{34}} = 2p_3g_3g_2p_3 + 2p_3g_3g_3p_2, \qquad \frac{\partial \Delta G}{\partial A_{35}} = 2p_3g_3g_1p_3 + 2p_3g_3g_3p_1,$$
$$\frac{\partial \Delta G}{\partial A_{36}} = 2p_3g_3g_1p_2 + 2p_3g_3g_2p_1, \qquad \frac{\partial \Delta G}{\partial A_{44}} = 2p_2g_3g_2p_3 + p_2^2g_3^2 + p_3^2g_2^2,$$
$$\frac{\partial \Delta G}{\partial A_{55}} = 2p_1g_3g_1p_3 + p_1^2g_3^2 + p_3^2g_1^2, \qquad \frac{\partial \Delta G}{\partial A_{66}} = 2p_1g_2g_1p_2 + p_1^2g_2^2 + p_2^2g_1^2,$$
$$\frac{\partial \Delta G}{\partial A_{45}} = 2p_2g_3g_1p_3 + 2p_3g_2g_1p_3 + 2p_2g_3g_3p_1 + 2p_3g_2g_3p_1,$$
$$\frac{\partial \Delta G}{\partial A_{46}} = 2p_2g_3g_1p_2 + 2p_3g_2g_1p_2 + 2p_2g_3g_2p_1 + 2p_3g_2g_2p_1,$$
$$\frac{\partial \Delta G}{\partial A_{56}} = 2p_1g_3g_1p_2 + 2p_3g_1g_1p_2 + 2p_1g_3g_2p_1 + 2p_3g_1g_2p_1. \qquad (14)$$

The derivatives $\partial A_{\alpha\beta}/\partial A_{\alpha\beta,ijk}$ can be obtained from Eq.(9) if we substitute ϵ by $A_{\alpha\beta}$ and ϵ_{ijk} by $A_{\alpha\beta,ijk}$.

Inversion of synthetic data

We consider a Cartesian coordinate system with x- and y-axes horizontal and the positive z-axis vertical. The considered model and configuration of the synthetic experiment is the same as that of Zheng and Pšenčík (1999). The model box is specified as follows: x is in the interval $< -1.0, 1.0 >$, y in $< -1.0, 1.0 >$ and z in $< 0.0, 0.7 >$ km. The medium in the model box is vertically inhomogeneous, hexagonally symmetric, and it is specified by the following matrix of density normalized elastic parameters (in km^2/s^2)

$$\begin{pmatrix} 15.71 & 5.05 & 4.46 & 0.00 & 0.00 & 0.00 \\ & 15.71 & 4.46 & 0.00 & 0.00 & 0.00 \\ & & 13.39 & 0.00 & 0.00 & 0.00 \\ & & & 4.98 & 0.00 & 0.00 \\ & & & & 4.98 & 0.00 \\ & & & & & 5.33 \end{pmatrix}.$$

at the $z = 0.0$ km and by

$$\begin{pmatrix} 19.64 & 6.31 & 5.58 & 0.00 & 0.00 & 0.00 \\ & 19.64 & 5.58 & 0.00 & 0.00 & 0.00 \\ & & 16.74 & 0.00 & 0.00 & 0.00 \\ & & & 6.23 & 0.00 & 0.00 \\ & & & & 6.23 & 0.00 \\ & & & & & 6.66 \end{pmatrix}.$$

at $z = 1.0$ km. The axis of symmetry (specified as vertical in the above matrices) is rotated by 80^o from vertical and by 25^o from the x-axis in the considered model.

We consider a synthetic multi-azimuthal multiple-source offset VSP experiment. The borehole is situated in the coordinate origin. There are 13 receivers distributed evenly within the borehole, They are distributed with the step of 0.05 km starting at the depth of 0.1 km. The effects of the free surface are neglected. Six profiles, 0^o, 30^o, 60^o, 90^o, 120^o and 150^o (measured counterclockwise from the x-axis) intersecting at the mouth of the borehole are considered. There are 9 evenly distributed sources on each profile on each side of the borehole, see the bottom part of Figure 1. The closest source is situated 0.1 km from the borehole, the step between the sources is also 0.1 km. In this way, we have 1404 qP wave travel time measurements at our disposal. In the upper part of Figure 1 straight lines connecting sources and receivers (and simulating rays) situated in the (x, z) plane are shown. We can see that the "ray" angular coverage at the top of the model is rather good. The shallowest receiver is illuminated both by nearly horizontal "rays" (from the most distant sources) and by nearly vertical "rays" (from the sources closest to the borehole). The situation at the deepest receivers is not so good. The deepest receivers are illuminated well by nearly vertical "rays" but there are no horizontal and nearly horizontal "rays" illuminating these receivers. We must therefore expect worse results of inversion for the deeper part of the model. The "observed" travel times for the described configuration were picked from synthetics calculated by a modified version of the ANRAY program package, see Gajewski and Pšenčík (1990).

We seek the values of elastic parameters ϵ_{ijk} at the corners of the model box. Variation of the parameters inside the box is trilinear, see Eq.(5). No additional assumption about inhomogeneity and/or anisotropy of the model is made. Thus, 15 WA parameters are sought in the first step of the inversion and all 21 elastic parameters are sought in subsequent inversion steps at each of the 8 corners of the model box. Since the number of sought parameters is 8x21, i.e., 168, and the number of "observations" is 1404, the inverse problem is sufficiently overdetermined. In the present experiment the travel time data were inverted without taking into account any error in their picking.

The starting model before the first iteration is vertically inhomogeneous and isotropic. Its P wave velocities were guessed from the data and given configuration. At the top of the model, the P velocity is 3.82 km/s, at the bottom 4.86 km/s. The corresponding S wave velocities were obtained from the above values by dividing them by $\sqrt{3}$. For all the higher iterations, the model is assumed to be generally inhomogeneous and anisotropic. The SVD technique is used for solving the system of linear equations resulting from the condition of minimization of the object function (1). Synthetic travel times between sources and receivers in an inhomogeneous isotropic medium and inhomogeneous anisotropic media are again calculated by a modified version of the ANRAY program package, see Gajewski and Pšenčík (1990).

The convergence of the iterative process is rather slow. We explain by insufficient illumination of the bottom part of the model. Figure 2 shows the variation of root mean square misfit of observed and synthetic travel times with increasing number of iterations. We can see that the misfit stops to vary only after about 50 iterations.

Figures 3 and 4, show sections of phase velocities for the exact model (red curve), initial model (black horizontal line), 1st, 2nd, 3rd and 10th iteration (black curves) and for the 82nd iteration (green curve). The matrices of elastic parameters at the top and the bottom of the model box, used for the generation of Figures 3 and 4, were obtained by averaging the values obtained at the four top and the four bottom corners of the model box. The differences between the four values were negligible. It means that the inversion did not introduce any false lateral gradient into the model.

The (x, z) sections of the qP wave phase velocity surfaces at the top and bottom of the model box are shown in the top and bottom plots of Figure 3, respectively. Figure 4 shows (y, z) sections of the qP wave phase velocity in the same display. We can see in all plots that the result of inversion corresponds very well to the exact qP wave phase velocity. At the same time, we can see that the convergence to the exact model at the top of the model is more rapid than at the bottom, see especially Figure 3. This is a consequence of the above mentioned problems with illumination of the bottom part of the model. We can also see that even iterations higher than one lead to significant changes in behaviour of phase velocities. Using only the first iteration, as, for example, Jech & Pšenčík (1992) did, would thus lead to incomplete results. Nevertheless, the most dramatic change in behaviour of phase velocity always occurs during the first iteration from vertically inhomogeneous isotropic medium to the inhomogeneous anisotropic medium.

In order to estimate the effect of the choice of the starting model, we considered another starting model, which was homogeneous and isotropic. After about 50 iterations, we arrived to the same results as shown above.

For making conclusions concerning the overall angular behaviour of phase velocities, the above sections are insufficient. In Figures 5 and 6 we show, therefore, continuous angular distribution of phase velocities at the top of the model box (Fig.5) and on the bottom of the model box (Fig.6). The upper plot in each figure shows the qP wave phase velocity corresponding a true matrix of elastic parameters, the bottom plot shows the velocity correspoinding to inverted matrix of elastic parameters. All plots were obtained using the approximate formula (3) with the WA parameters specified from the respective matrix of elastic parameters. The qP wave phase velocity values are shown in a plot covering azimuthal and polar angles between 0^o and 180^o. In fact, a lower halpsphere is shown in Figs.5 and 6. The vertical line with the azimuth of 0^o corresponds to the (x, z) section shown by red (true) or green (inverted) line in Figure 3, the vertical line with the azimuth of 90^o corresponds to the (y, z) section shown in Figure 4. Polar angle 0^o corresponds to a horizontal direction, 90^o to vertical direction. The phase velocities are shown by isolines on the gray scaled background. The gray scale is used to indicate the variation of phase velocities between isolines. We can see from Figures 5 and 6 that an overall fit of the inverted and true phase velocities is very good. As expected, slightly larger differences can be observed for the bottom of the model, see Figure 6.

With the above described iterative process we succeeded to determine spatial variation of a complete matrix of elastic parameters although we used only qP wave travel times. It is of interest to see how well phase velocities of qS waves are determined from such an experiment. In Figures 7, 8 and 9, 10 we show sections of phase velocities of $qS1$ and $qS2$ waves for the exact model (red curve), 1st iteration (blue curve), 2nd, 3rd, 4th and 10th

iteration (black curves) and for the 82nd iteration (green curve). We can see that the resulting phase velocities are systematically underestimated. The azimuthal dependence of the exact (red) curve and the resulting (green) curve is very similar, both curves being shifted by a constant value. The results shown in Figures 7-10 were obtained with assumptions (10) and (11). Perhaps a different assumption could lead to better results.

Tests with a varying size of the model box and with a gradient method instead of SVD have shown independence of the procedure on the size of the model considered and on the method used to solve the system of linear equations resulting from the condition of minimization of the object function.

Conclusion and discussion

Inversion for all 21 elastic parameters from qP wave travel time observations only, starting from a vertically inhomogeneous or a homogeneous isotropic model proved to be feasible. Inversion consisted of two separate steps. First step from isotropy to anisotropy yielded only 15 WA parameters, see Eq.(4). All 21 elastic parameters were then obtained in subsequent iterations from anisotropic starting model to an updated anisotropic model. It turned out that although the first step yielded results whose basic features remained preserved during subsequent iterations, results of the first iteration still differ significantly from the final results. This implies that higher iterations should be used generally. Tests have shown that acceptable results of inversion depend only slightly on the choice of the starting background isotropic model.

The described procedure has been also applied to experimental data from a vicinity of the Underground Research Laboratory (URL) in Manitoba, see Liu et al. (1999). That experiment confirmed our speculations about the low convergence of the iterative process due to insufficient illumination of the studied medium. In the URL experiment extremaly good ray coverage of studied region was available. The misfit of the observed and synthetic travel times stopped to vary after 7th iteration in this case.

The proposed method needs an extensive testing in near future. We plan further tests on sensitivity of the procedure to the choice of a background. Until now we worked with noise-free data. We would like to test the sensitivity of the procedure to data containing various levels of noise. Tests of the relation of the convergence rate and illumination should be performed. The tests should also investigate sensitivity of results to a reduced number of profiles and sources along them. As indicated in the text, a study must be performed, which would show whether alternative assumptions to assumptions (10) and (11) would lead to better inversion results for qS waves. One of the principal questions of tomography in inhomogeneous anisotropic media is whether inhomogeneity can transform into anisotropy and vice versa during an inversion. The tests presented by Jech and Pšenčík (1992) and tests presented in this contribution seem to indicate that inhomogeneity can be recovered unaffected by anisotropy and vice versa. The models considered by Jech and Pšenčík (1992) and here are, however, very simple. Therefore, tests with more complicated laterally varying anisotropic media are necessary.

Acknowledgements

The authors thank Leonardo Martins for his help with generating Figs.5 and 6 and Xuyao Zheng for useful comments. This work was supported by the consortium project "Seismic waves in complex 3-D structures (SW3D)" and by the Brazilian Ministry of Science and Technology Pronex - Engenharia de Petróleo.

References

Aggio,A.S., 1995. Inversion of qS and qP waves from VSP data in 3D heterogeneous anisotropic media with hexagonal or orthorhombic symmetry. PhD thesis, UFBa Salvador, Brazil (in Portuguese).

Červený,V., 1982. Direct and inverse kinematic problems for inhomogeneous anisotropic media - a linearization approach. *Contr. Geophys. Inst. Slov. Acad. Sci.*, **13**, 127-133.

Chapman,C.H. & Pratt,R.G., 1992. Traveltime tomography in anisotropic media-I. Theory. *Geophys.J.Int.*, **109**, 1-19.

Gajewski,D. & Pšenčík,I., 1990. Vertical seismic profile synthetics by dynamic ray tracing in laterally varying layered anisotropic structures. *J.geophys.Res.*, **95**, 11301-11315.

Jech,J. & Pšenčík,I., 1989. First-order perturbation method for anisotropic media. *Geophys.J.Int.*, **99**, 369-376.

Jech,J. & Pšenčík,I., 1992. Kinematic inversion for qP and qS waves in inhomogeneous anisotropic structures. *Geophys.J.Int.*, **108**, 604-612.

Liu,J., Pšenčík,I. & Young,P., 1999. Inversion of qP wave travel times from the URL experiment. Preprint, Geophysical Inst. AS CR.

Maxwell,S.C. & Young,R.P., 1995. A controlled in-situ investigation of the relationship between stress, velocity and induced seismicity. Geophys. Res. Letters., **22**, 1049-1052.

Pšenčík,I. & Gajewski,D., 1998. Polarization, phase velocity and NMO velocity of qP waves in arbitrary weakly anisotropic media. *Geophysics*, **63**, 1754-1766.

Zheng,X. & Pšenčík,I., 1998. Determination of weak anisotropy parameters from the qP wave slowness and particle motion measurements in laterally homogeneous media. In: Seismic Waves in Complex 3-D Structures, Report 8, pp. 47-62, Dept.of Geophysics, Charles University Prague.

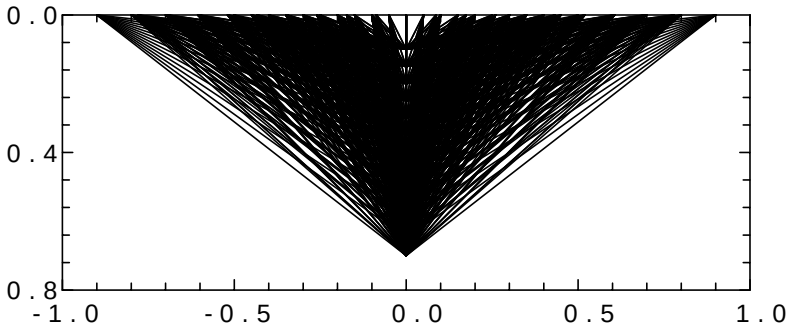

Straight-line connections
of source-receiver pairs in (x,z) plane

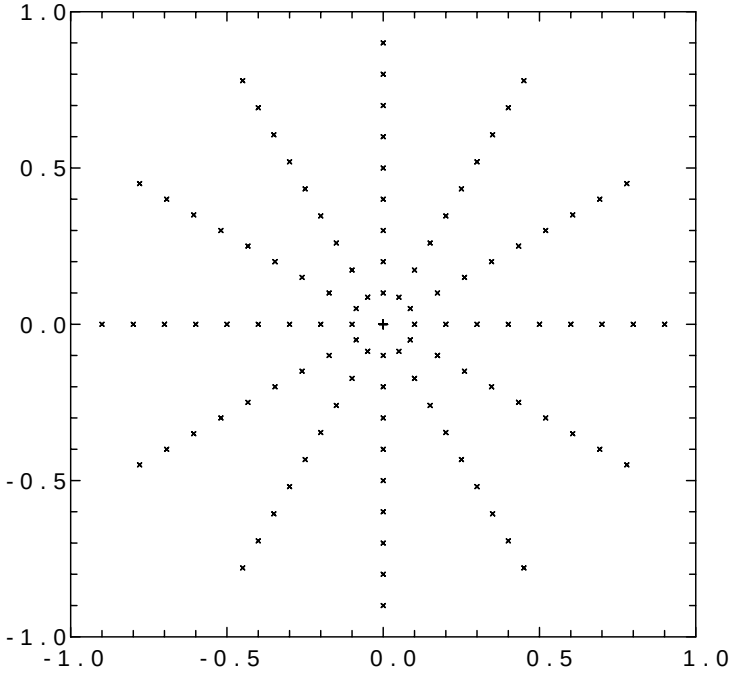

Position of sources and the borehole in (x,y) plane

Figure 1

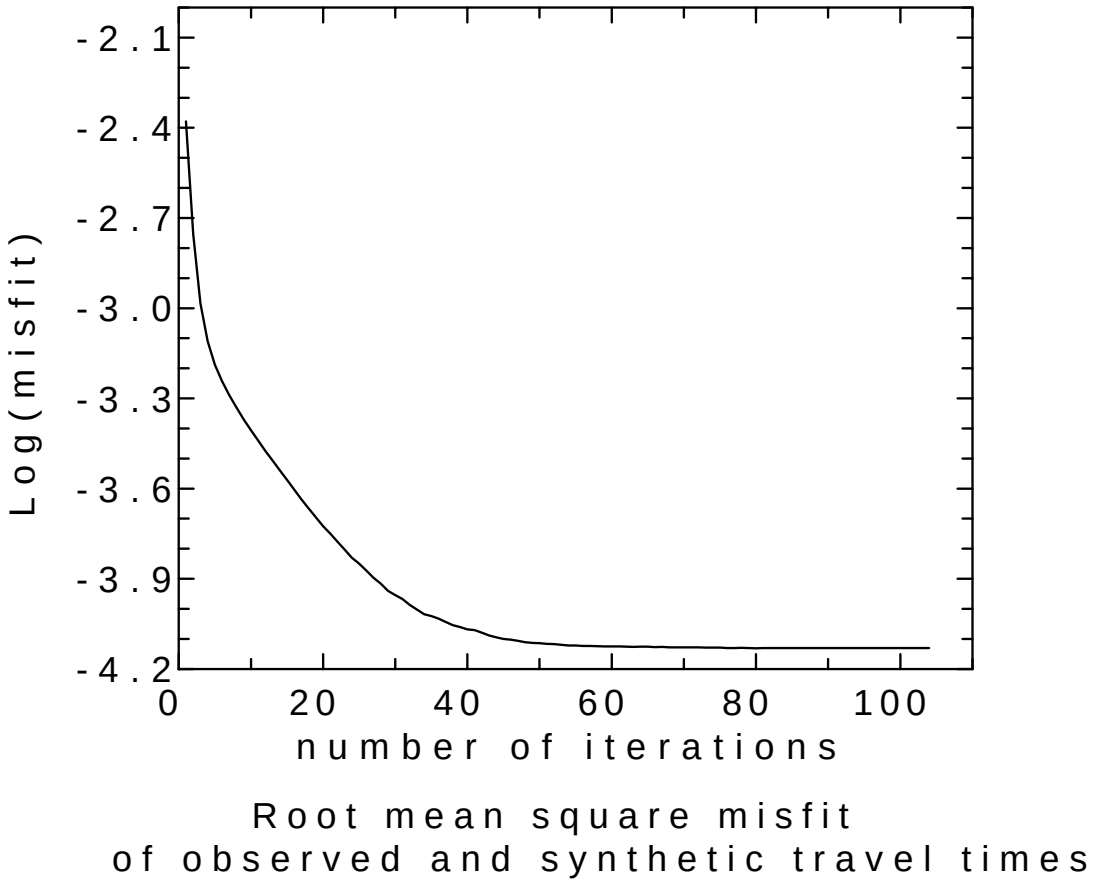
-2.1
-2.4
-2.7
-3.0
-3.3
-3.6
-3.9
-4.2
Log(misfit)
0
20
40
60
80
100
number of iterations
Root mean square misfit
of observed and synthetic travel times

Figure 2

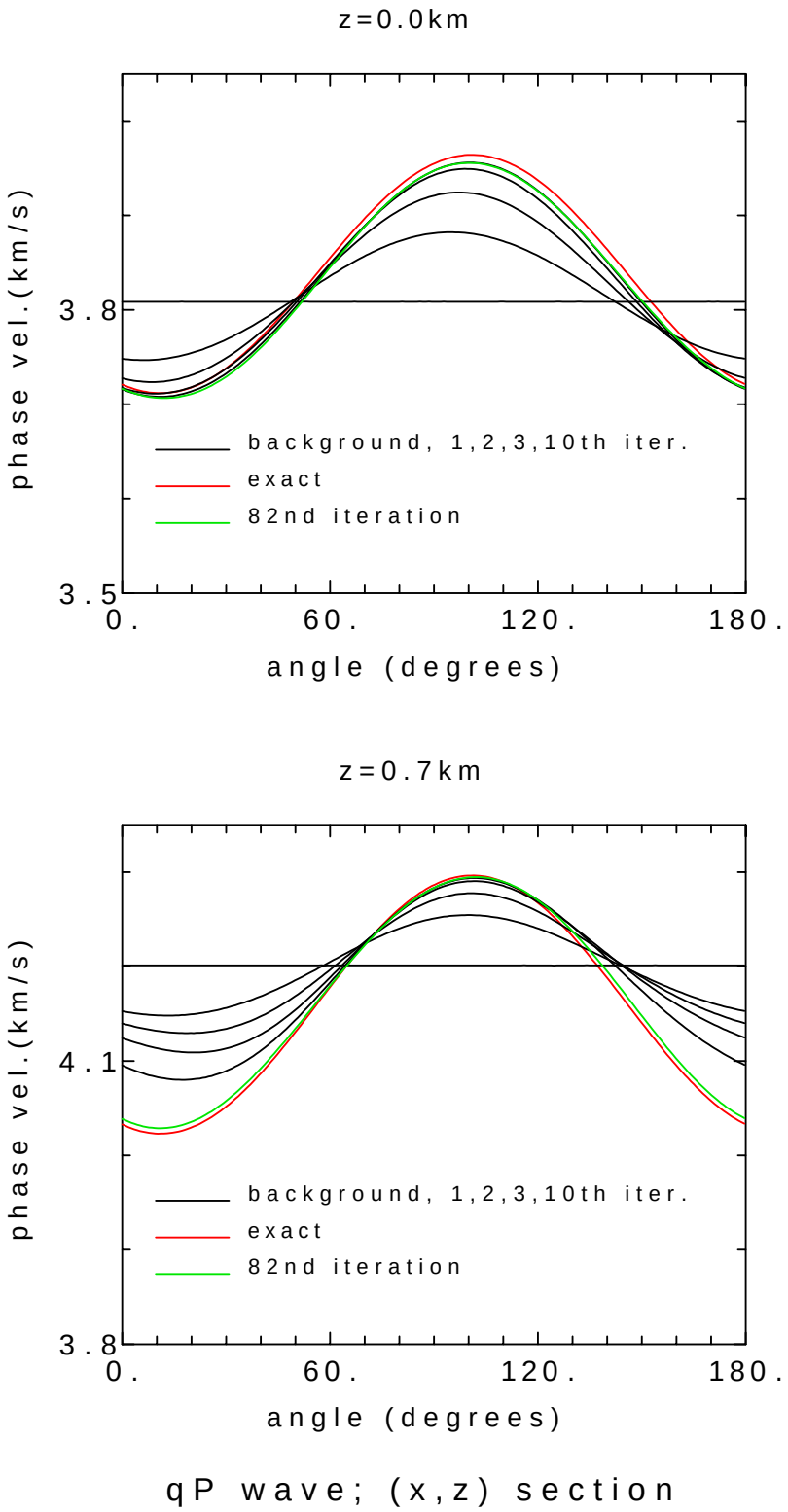
z=0.0km
phase vel.(km/s)
3.8
3.5
0.
60.
120.
180.
angle (degrees)
background, 1,2,3,10th iter.
exact
82nd iteration
z=0.7km
phase vel.(km/s)
4.1
3.8
0.
60.
120.
180.
angle (degrees)
background, 1,2,3,10th iter.
exact
82nd iteration
qP wave; (x,z) section

Figure 3

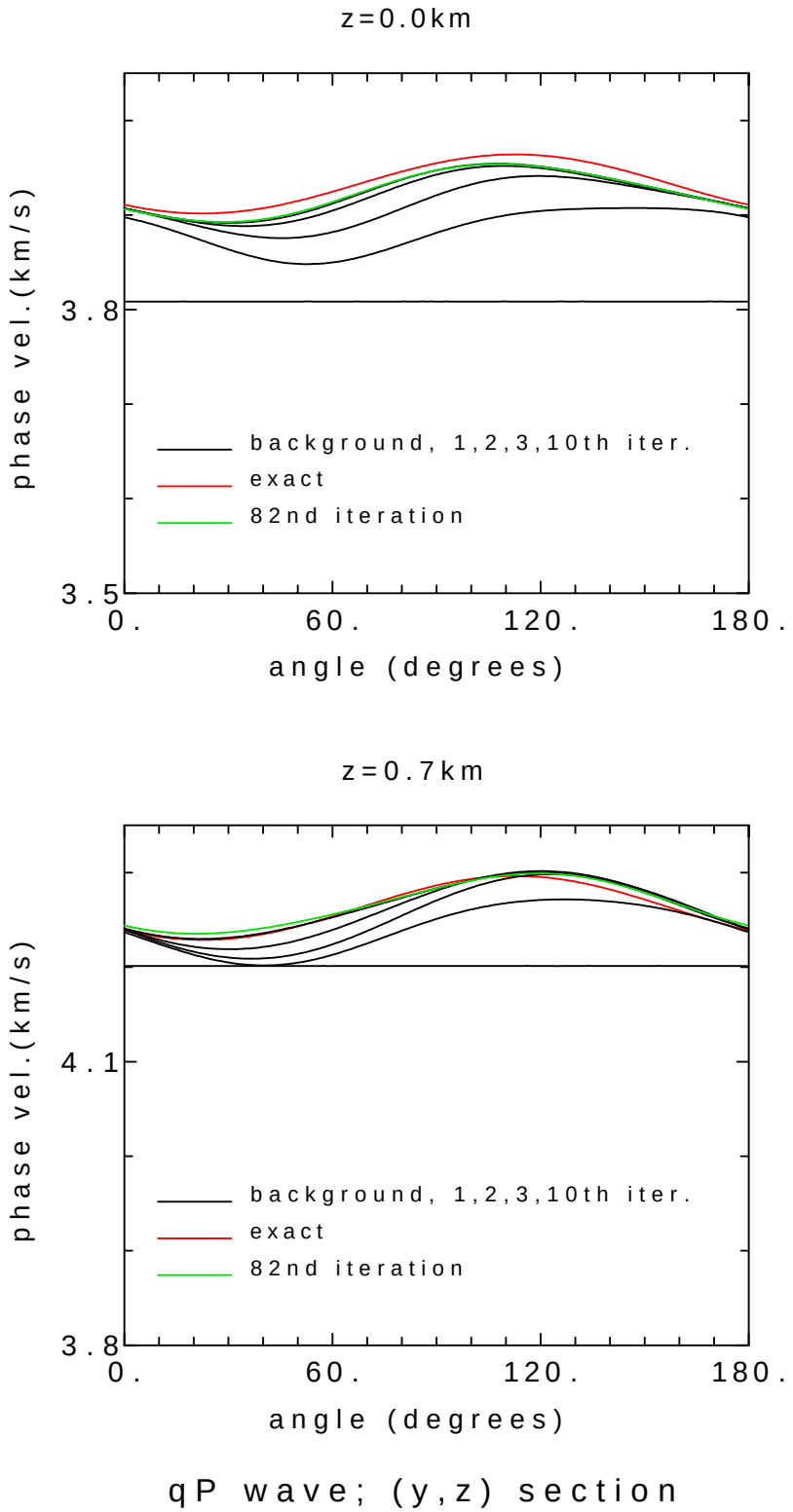
z=0.0km
phase vel.(km/s)
3.8
3.5
0.
60.
120.
180.
angle (degrees)
background, 1,2,3,10th iter.
exact
82nd iteration
z=0.7km
phase vel.(km/s)
4.1
3.8
0.
60.
120.
180.
angle (degrees)
background, 1,2,3,10th iter.
exact
82nd iteration
qP wave; (y,z) section

Figure 4

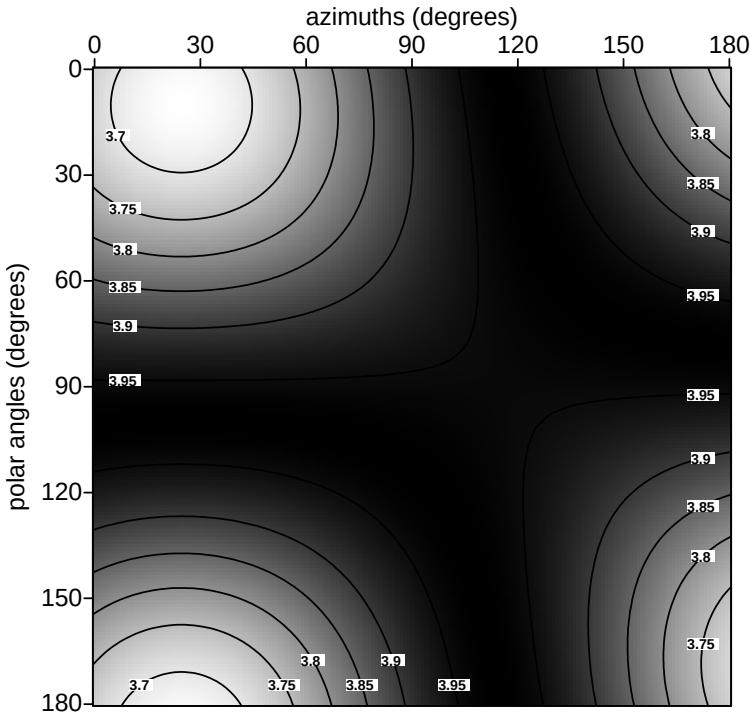

qP wave phase velocity: exact

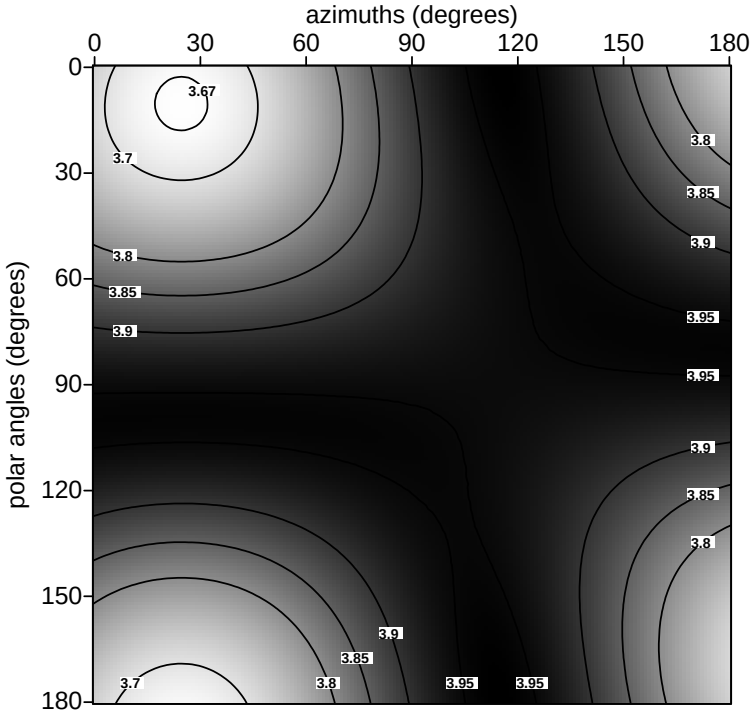

qP wave phase velocity: inverted

Figure 5

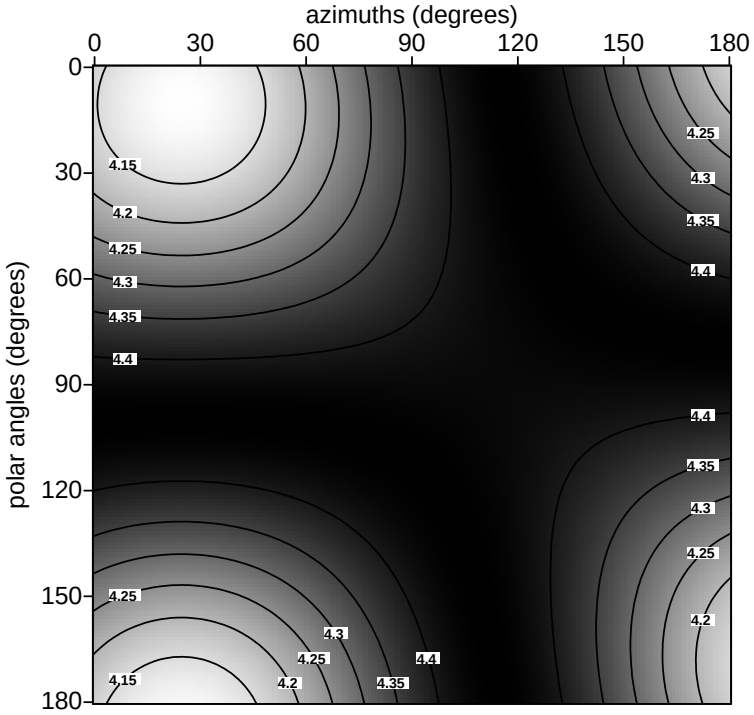

qP wave phase velocity: exact

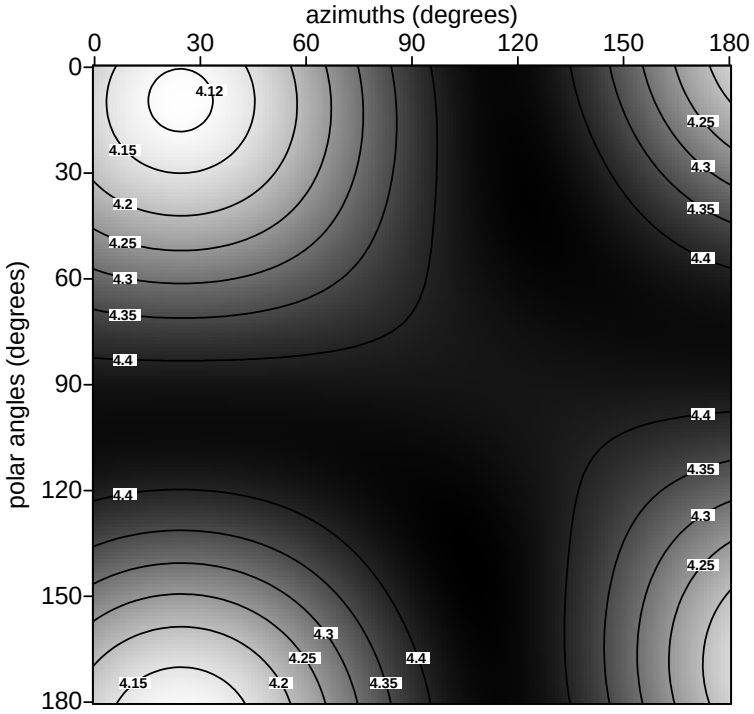

qP wave phase velocity: inverted

Figure 6

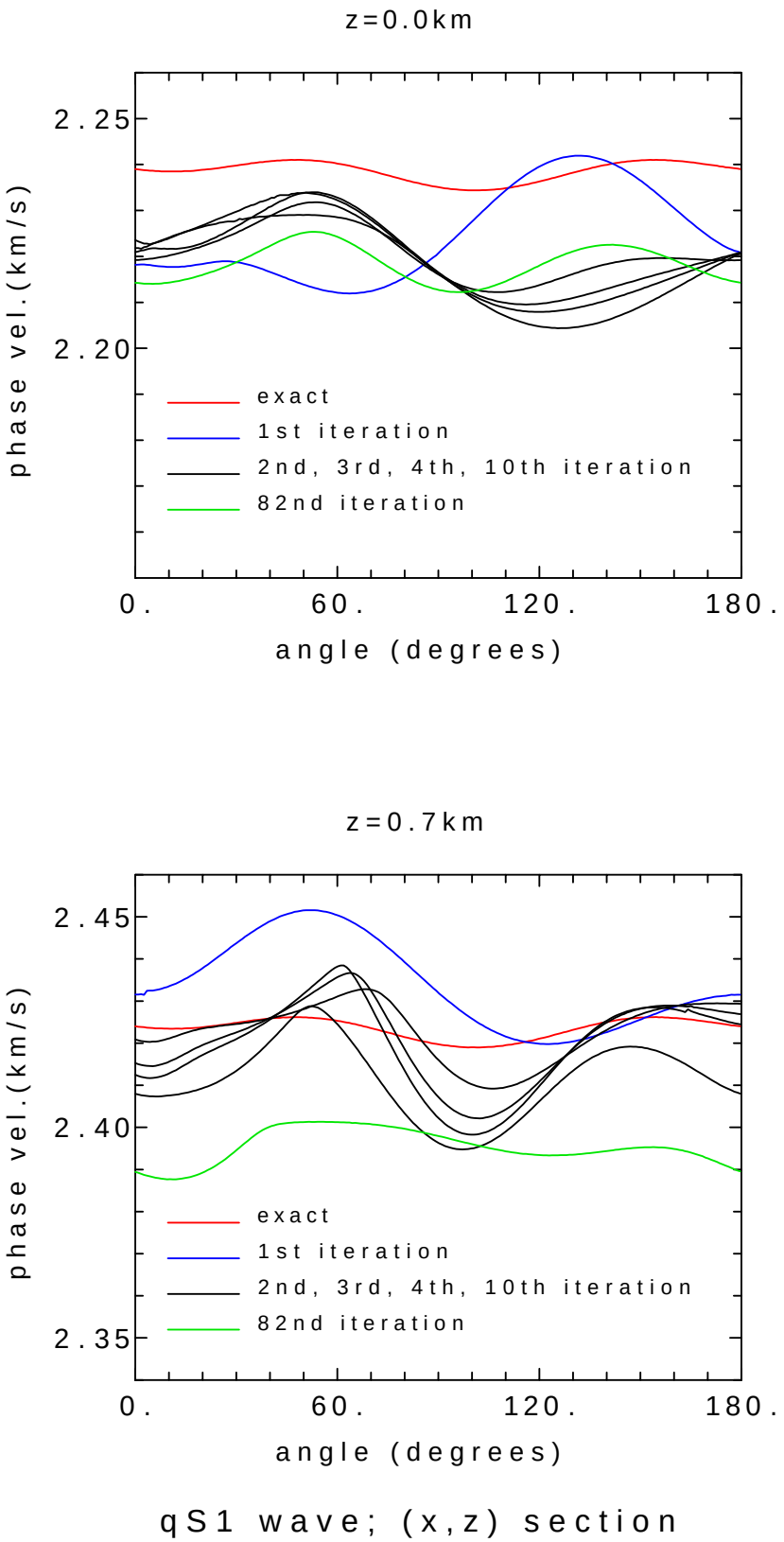
z=0.0km
2.25
2.20
phase vel.(km/s)
exact
1st iteration
2nd, 3rd, 4th, 10th iteration
82nd iteration
0.
60.
120.
180.
angle (degrees)
z=0.7km
2.45
2.40
2.35
phase vel.(km/s)
exact
1st iteration
2nd, 3rd, 4th, 10th iteration
82nd iteration
0.
60.
120.
180.
angle (degrees)
qS1 wave; (x,z) section

Figure 7

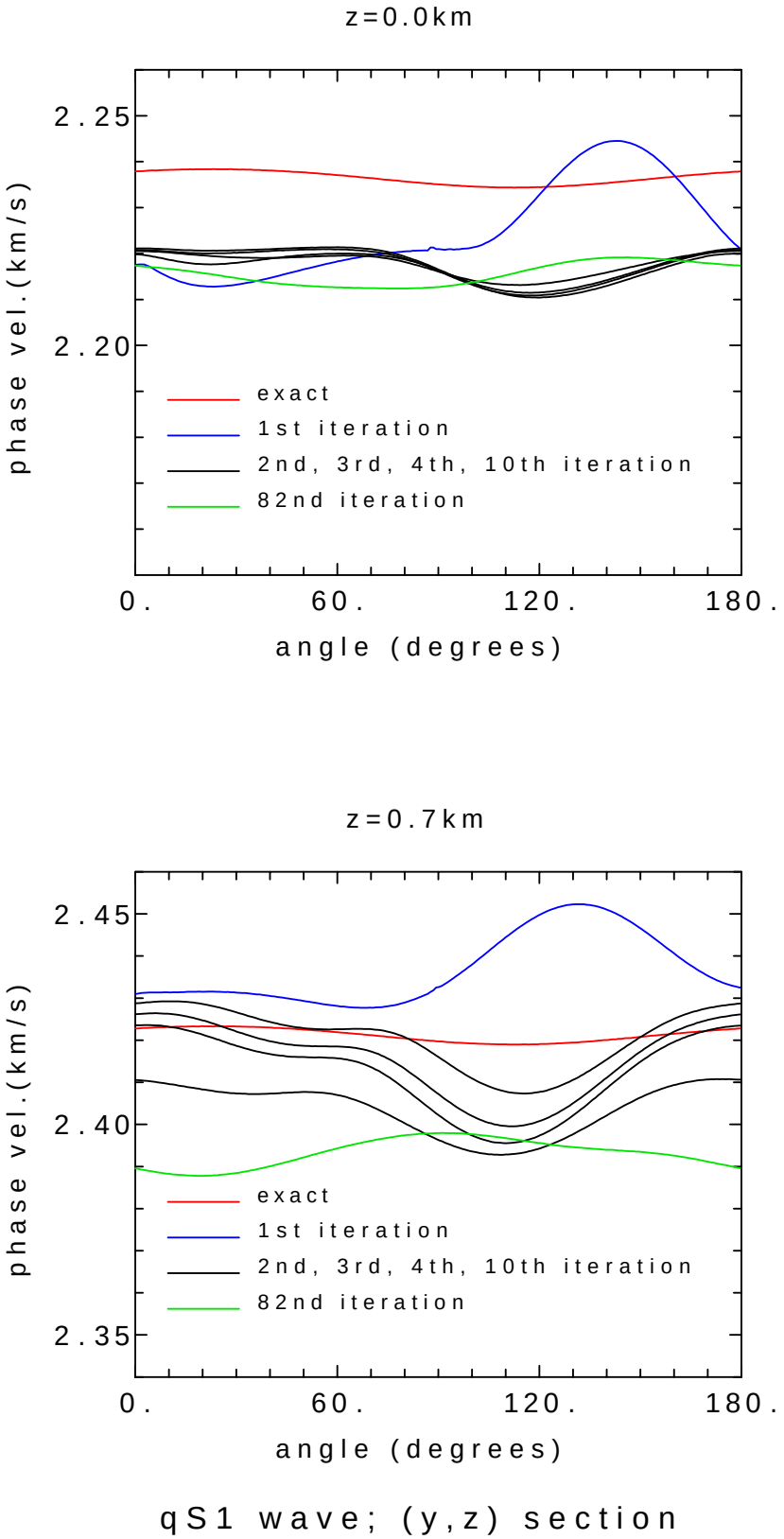
z=0.0km
2.25
2.20
phase vel.(km/s)
exact
1st iteration
2nd, 3rd, 4th, 10th iteration
82nd iteration
0.
60.
120.
180.
angle (degrees)
z=0.7km
2.45
2.40
2.35
phase vel.(km/s)
exact
1st iteration
2nd, 3rd, 4th, 10th iteration
82nd iteration
0.
60.
120.
180.
angle (degrees)
qS1 wave; (y,z) section

Figure 8

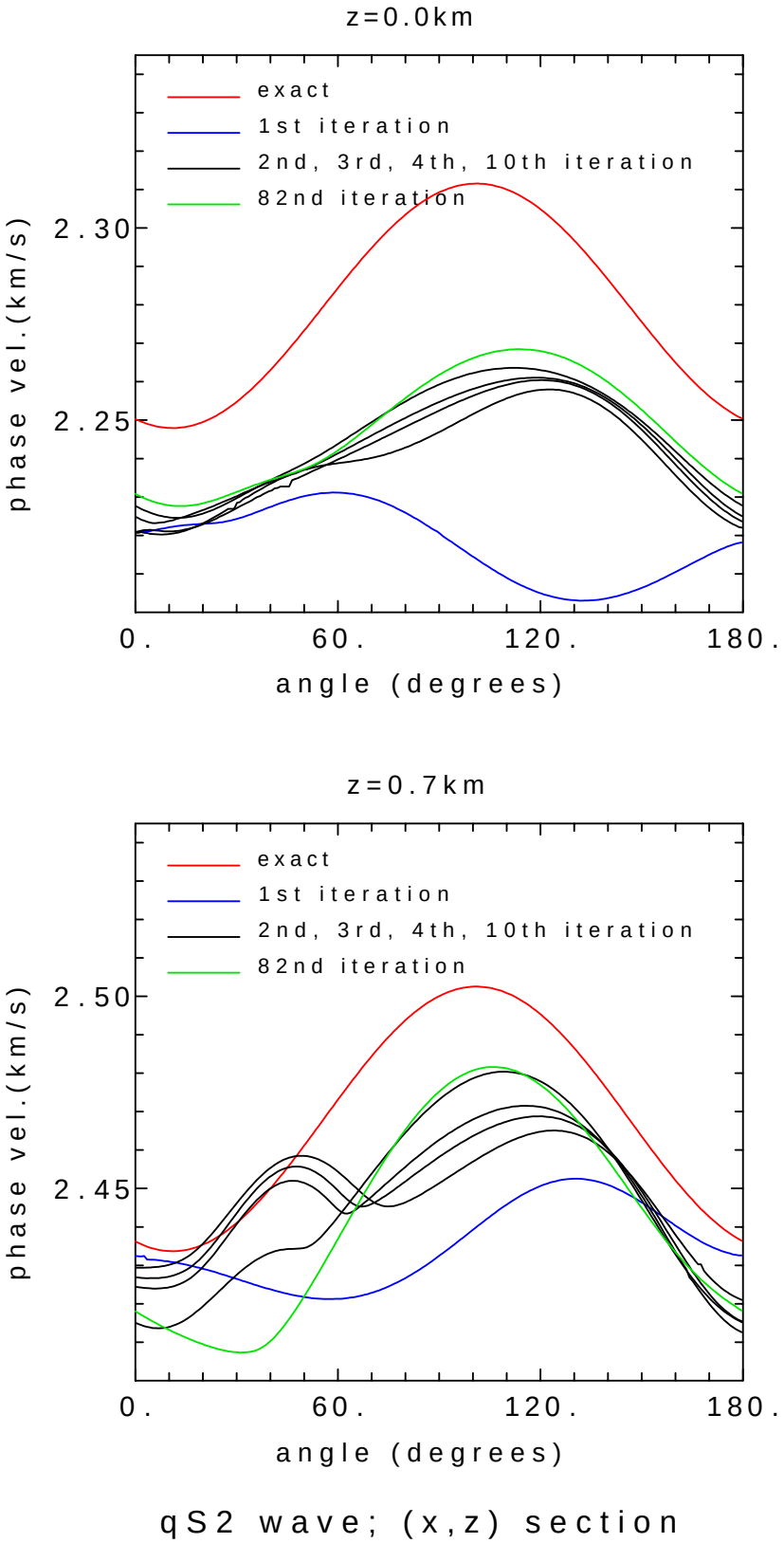
z=0.0km
exact
1st iteration
2nd, 3rd, 4th, 10th iteration
82nd iteration
phase vel.(km/s)
2.30
2.25
0.
60.
120.
180.
angle (degrees)
z=0.7km
exact
1st iteration
2nd, 3rd, 4th, 10th iteration
82nd iteration
phase vel.(km/s)
2.50
2.45
0.
60.
120.
180.
angle (degrees)
qS2 wave; (x,z) section

Figure 9

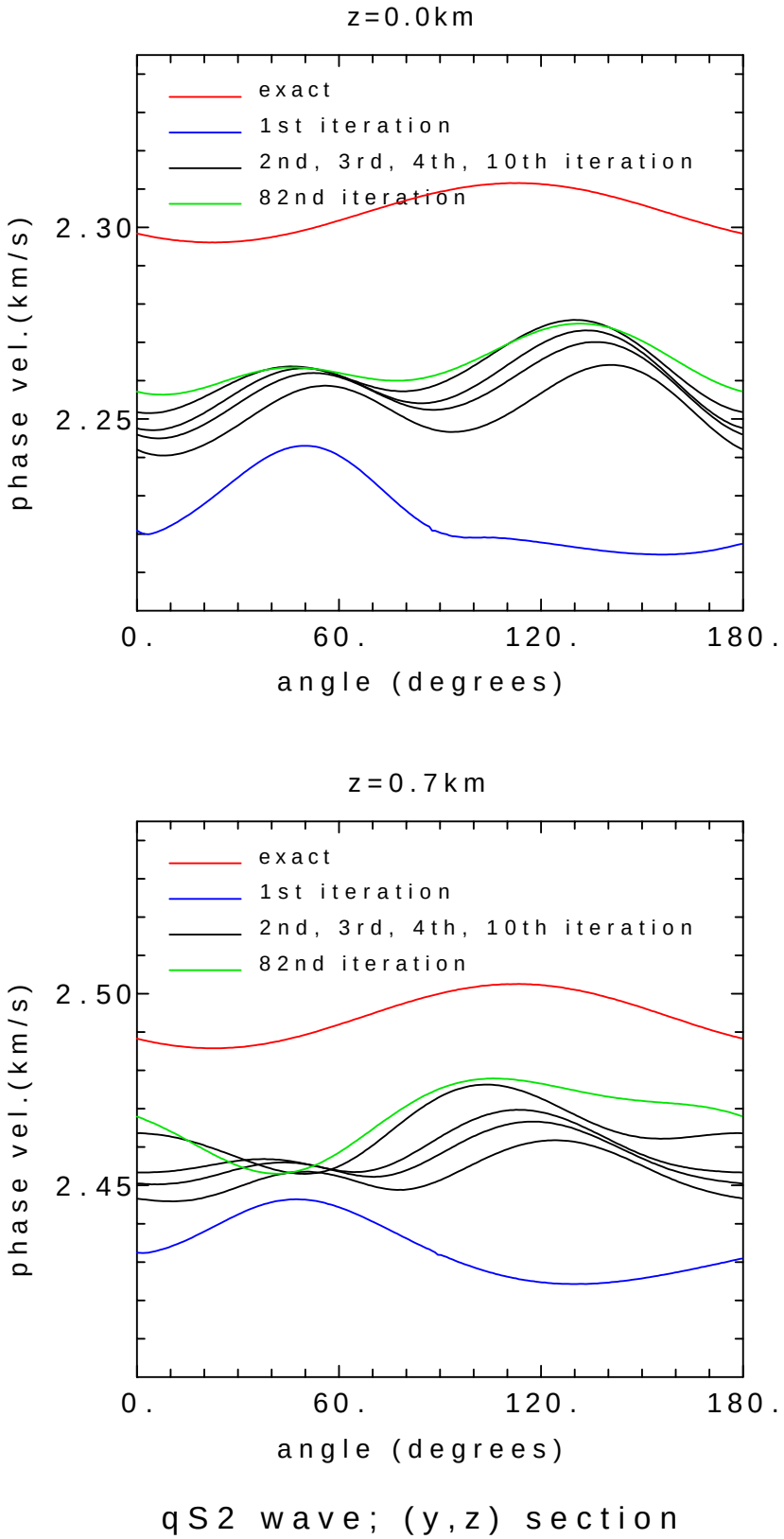
z=0.0km
exact
1st iteration
2nd, 3rd, 4th, 10th iteration
82nd iteration
2.30
2.25
phase vel.(km/s)
0.
60.
120.
180.
angle (degrees)
z=0.7km
exact
1st iteration
2nd, 3rd, 4th, 10th iteration
82nd iteration
2.50
2.45
phase vel.(km/s)
0.
60.
120.
180.
angle (degrees)
qS2 wave; (y,z) section

Figure 10